Penetration of high intensity focused ultrasound *in vitro* and *in vivo rabbit brain* using MR imaging.

Venediktos Hadjisavas ,Christakis Damianou, Kleanthis Ioannides,
Nicos Mylonas, Andreas Couppis, Panayiotis A. Kyriacou, Dimitris Iosif, Theodoros HadjiCharalambous,
Gavriella Parea.

Abstract—**In this paper magnetic resonance imaging (MRI) is investigated for monitoring the penetration of high intensity focused ultrasound (HIFU) *in vitro* and *in vivo* rabbit brain. A single element spherically focused transducer of 5 cm diameter, focusing at 10 cm and operating at 2 MHz was used. A prototype MRI- compatible positioning device is described. MRI images were taken using fast spin echo (FSE). The length of the lesions *in vivo* rabbit brain was much higher than the length *in vitro*, proving that the penetration in the *in vitro* brain is limited by reflection due to trapped bubbles in the blood vessels.**

I. INTRODUCTION

Thermal ablation of brain in animals with high intensity focused ultrasound (HIFU) was very popular in the 50's and 60's [1-2]. HIFU was used in the clinical setting by Fry and Johnson [3] and showed that HIFU had the potential to treat brain cancer. Several groups used hyperthermia (heating of several minutes at 43 ^{o}C) to treat brain tumours [4-5]. Such clinical trials were abandoned probably due to the inexistence of effective imaging modalities to guide the therapy. Especially for the case of brain it is extremely important to have absolute control of the ablation in order to avoid vital brain tissue damage such as the neurons. Now with the advancement of HIFU technology guided by magnetic resonance imaging (MRI), it will be possible to conduct clinical studies for brain cancer.

Since 1994 several studies by the group of Dr. Hynynen [6-11] demonstrated the creation of lesions in animal brain using MRI for monitoring. However, in these studies only pure thermal lesions were shown. Also in the above studies the production of well-controlled large lesions was never demonstrated. In this paper we have explored extensively the use of MRI to image both lesions created under thermal and cavitation or boiling mechanisms. Also in this paper we demonstrate the creation of well controlled large thermal and bubbly lesions. Another issue that was never demonstrated in previous studies is the lesion penetration deep in tissue, an issue which is also explored in this paper for *in vitro* and *in vivo* exposures.

Currently there is a HIFU system which is guided by MRI developed by Insightech which treads fibroids [12]. This system which is already FDA approved has been deployed in 30 locations worldwide. Therefore, HIFU guided by MRI, opens the possibility for treating tumors in other organs.

A single element spherically focused transducer of 5 cm diameter, focusing at 10 cm and operating at 2 MHz was used. The transducer was scanned in a 3-d grid using an MRI compatible mechanical positioning device. The positioning device designed is simple, cost effective, portable and universal. By universal we mean that it can be used in any MRI scanner available, since it is placed on the table of the MRI scanner and therefore integration with all MRI scanners is possible. Also the current device includes a flexible coupling system, and thus it can be used in all the anatomies accessible by HIFU (liver, kidney, breast, brain and pancreas). For both *in vitro* and *in vivo* experiments we have used New Zealand rabbits.

In this paper the goal was to investigate the effectiveness of MRI to monitor therapeutic protocols of HIFU in the brain. For such investigation, we have used the basic pulse sequences T1-w and T2-w fast spin echo (FSE). These MRI pulse sequences have been successful in other organs regarding their ability to identify thermal lesions. For example in muscle the contrast of lesions was investigated by Hynynen et al. [13], in kidney by Hynynen et al. [14], and Damianou et al. [15], in liver by Rowland et al. [16], and in prostate by Rouviere et al. [17], and by Pisani et al. [18].

II. MATERIALS AND METHODS

A. HIFU/MRI SYSTEM

Fig. 1 shows the block diagram of the HIFU/MRI system which includes the following subsystems: 1) HIFU system, 2) MR imaging, 3). Positioning device (robot) and associate drivers. A brief description of each of the subsystems flows below.

1). HIFU system: The HIFU system consists of a signal generator (HP 33120A, Agilent technologies, Englewood, CO, USA), a RF amplifier (250 W, AR, Souderton, PA, USA), and a spherically shaped bowl transducer made from piezoelectric ceramic of low magnetic susceptibility (Etalon, Lebanon, IN, USA). The transducer operates at 2 MHz, has focal length of 10 cm and diameter of 5 cm. The transducer

C. Damianou is with Frederick University Cyprus, Nicosia, Cyprus and MEDSONIC LTD, Limassol, Cyprus (phone: +357-99-471977; fax: +357-25735001; e-mail: cdamianou@cytanet.com.cy).
P. Kyriacou is with City University, London, UK (phone: +44 (0)20 7040 8131; fax: +44 (0)20 7040 8568; e-mail: p.kyriacou@city.ac.uk).
V. HadjiSavvas is with City University, London, UK and Frederick University Cyprus, Nicosia, Cyprus.
K. Ioannides is with Polikliniki Igia, Limassol, Cyprus
N. Milonas, and A. Couppis are with City University, London, UK and Frederick University Cyprus, Nicosia, Cyprus.
D. Iosif is with Frederick University Cyprus, Nicosia, Cyprus.
Theodoros HadjiCharalambous and Gavriella Parea are with MEDSONIC LTD, Limassol, Cyprus.

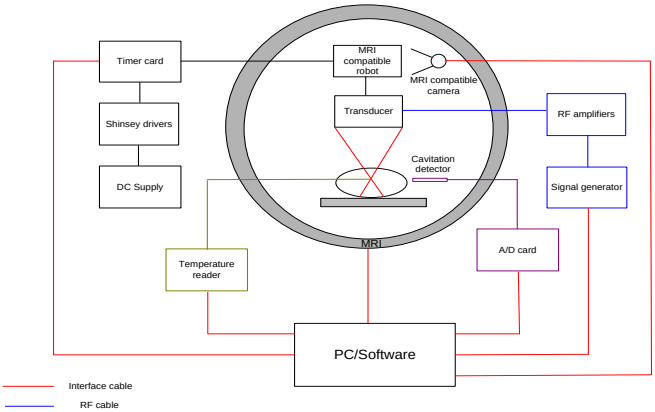

Fig. 1. HIFU system under MRI guidance showing the various functionalities of the HIFU/MRI system.

is rigidly mounted on the MRI-compatible positioning system (MEDSONIC LTD, Limassol, Cyprus).

2). MRI Imaging: The 3-d positioning device and the transducer were placed inside a MRI scanner (Signa 1.5 T, by General Electric, Fairfield, CT, USA). A spinal coil (USA instruments, Cleveland, OH, USA) was used.

3). Positioning device:

3.1). Description of the mechanical design: The robot has been developed initially for three degrees-of-freedom, but it can be easily developed for 5 degrees of motion. Since the positioning device is placed on the table of the MRI scanner its height should be around 55 cm (bore diameter of the MRI scanner). The length of the positioning device is 45 cm and its width 30 cm. The weight of the positioning device is only 6 kg and therefore it can be considered as portable.

Fig. 2.A shows the rectangular base of the positioning device made out of polyethylene. This plastic base holds the 3 stages that establish motion in the X, Y and Z direction. Four polyethylene angles are placed on the base. Two brass rods are attached to the 4 angles. A fixed polycarbonate pulley is supported on polyethylene angles through a plastic rod. A piezoelectric motor (USR60-S3N, Shinsei Kogyo Corp., Tokyo, Japan) is fixed on another polyethylene angle. A neoprene belt is placed around the fixed pulley and the pulley which is coupled to the motor. This figure shows also the water container that host the transducer. The transducer is immersed in the water container which is filled with degassed water or saline. The water is poured in a mylar bag. The mylar bag is made thin enough to conform to the contours of the target. A circular window is opened in the water container in order to allow ultrasound energy to be applied through the body. For the purpose of brain ablation, the head of the subject is placed inside an open MRI coil.

Fig. 2.B shows the bottom side of the polyethylene sheet that establishes motion in the X-direction. If the motor is energized, the belt which is coupled to this sheet will rotate, and eventually linear motion of this sheet is established. This sheet is coupled to the brass rods of the base (Fig. 2.A).

Fig. 2.C shows the rectangular sheet (top side) which is used to provide motion in the Y-axis. The same principles as in Fig. 2.A are implemented. The only difference is the smaller size of this sheet. Fig. 2.D shows the bottom side of the polyethylene sheet that establishes motion in the Y-direction.

Fig. 2.E shows the angle that carries the Z-stage. This angle is placed on the stage shown in Fig. 2.D. Fig. 2.F shows the rectangular sheet made out of polyethylene for moving the transducer in the Z axis (same principles are applied as in Fig. 2.A). Fig. 2.G shows the bottom side of the polyethylene sheet that establishes motion in the Z-direction.

Fig. 2.H shows the holder of the transducer. A plastic rod is attached on the Z –axis sheet. A brass rod is coupled to the plastic rod. The transducer holder is attached to the brass rod. The HIFU transducer is coupled to the holder. More details of this positioning device can be found in [19].

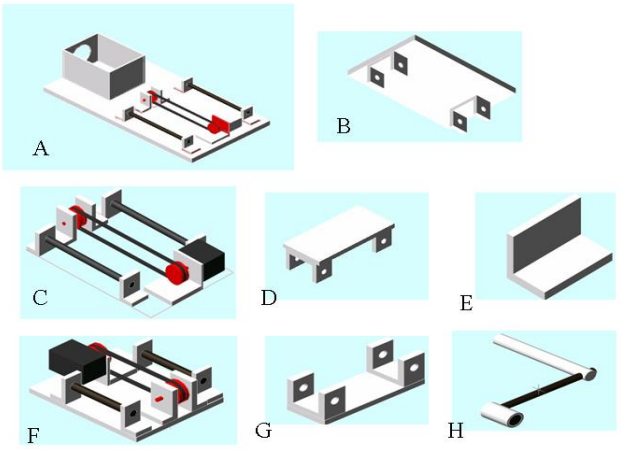

Fig. 2 Schematic of the robot showing all of its stages.

3.2). *Robot drivers:*

The box hosting the motor drivers is placed outside the MRI room since magnetic materials are involved. Fig. 3 shows the wiring diagram of the driving electronics and computer-controlled interface. A DC supply (24 V, 6 A) is used to drive the Shinsei drivers. Wires from the Shinsei drivers are connected to a PCI 6602 interface card (National instruments, Austin, Texas, USA) via a connecting block. The PCI 6602 interface card includes timing and digital I/O modules. The interface is connected in a PC (Dell Inc. Round Rock, Texas, USA).

The motors are driven when the ground and clockwise terminals of the Shinsei drivers are connected (clockwise rotation) or when the ground and anti-clockwise terminals of the Shinsei drivers are connected (anti -clockwise rotation). This is achieved by initiating a command from the software which places two digital output terminals of the PCI card (for example ground and clockwise) in the same potential. Movement of a certain axis can be achieved also manually by means of an ON-OFF-ON switch.

B. *In vitro experiments*

Various *in vitro* experiments were carried out using MRI to image the lesions created in brain tissue using HIFU.

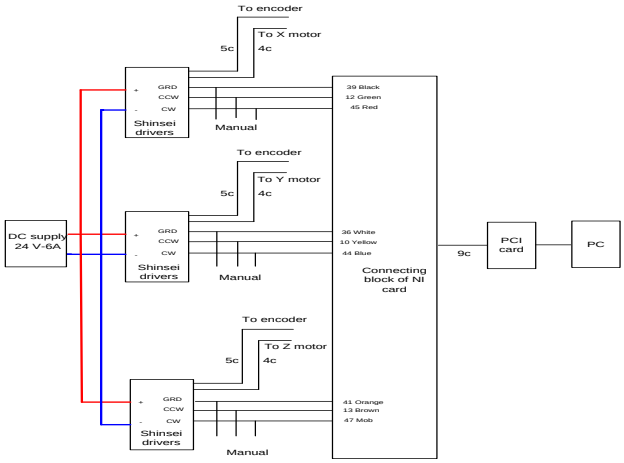

Fig. 3 the wiring diagram of the driving electronics and computer-controlled interface

The acoustical coupling depicted in Fig. 4.A was used for the *in vitro* experiments. In this method the tissue is placed outside the water container which is filled with degassed water. Due to the weight of the water container the coupling when using this method is excellent. This method can be described as a superior to inferior approach, meaning that the transducer is on top of the tissue. In the commercial system described by Stewart et al. [12] the approach used is inferior to superior, meaning that the transducer in below the tissue. Totally 4 rabbit brains were ablated.

C. *In vivo experiments*

In Fig. 4.B the approach used for acoustical coupling is lateral meaning that ultrasound propagates to the tissue either from left or right. This method is used to couple ultrasound to the rabbit brain in vivo. The tissue with this method has to be in good contact with the water container in order to achieve good coupling.

For the *in vivo* experiments, New Zealand adult rabbits were used weighting approximately 3.5-4 kg. Three rabbits were used in the experiments. The rabbits were anaesthetized using a mixture of 500 mg of ketamine (100 mg/mL, Aveco, Ford Dodge, IA), 160 mg of xylazine (20 mg/mL, Loyd Laboratories, Shenandoah, IA), and 20 mg of acepromazine (10 mg/mL, Aveco, Ford Dodge, IA) at a dose of 1 mL/kg.

The presence of the skull in the ultrasonic path not only distorts the field by reflection, but may also destroy the underlying tissue in contact with it by absorbing ultrasonic energy and dissipating it as heat. Therefore, a craniotomy was necessary in order to permit unimpeded passage of the cone of sound. The extent of the craniotomy depends on the solid angle of radiation and the depth of the target from the cranial surface. The larger the angle and the deeper the target, the larger the size of craniotomy needed. For the transducer used and a target depth of 1 cm, a circular craniotomy of 3 cm in diameter was adequate. The animal experiments protocol was approved by the national body in Cyprus responsible for animal studies (Ministry of Agriculture, Animal Services).

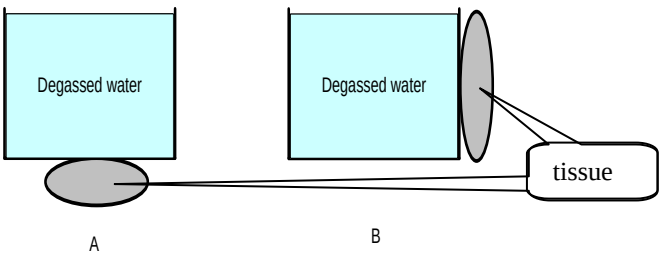

Fig. 4 Coupling method for A) *in vitro* experiments and B) *in vivo* experiments.

D. *HIFU parameters*

The *in situ* spatial average intensity was estimated based on the applied power and the half-power width of the beam of the transducer. The details of the intensity estimation can be found in [21]. In all the exposure, unless stated otherwise the ultrasound was turn on continuously for 20 s.

E. *MRI processing*

The following parameters were used for T1-W FSE: TR=500 ms, TE=9 ms, slice thickness=3 mm (gap 0.3 mm), matrix=256x256, FOV=16 cm, NEX=1, and ETL=8. For T2-W FSE: TR=2500 ms, TE=60 ms, slice thickness=3 mm (gap 0.3 mm), matrix=256x256, FOV=16 cm, NEX=1, and ETL=8. The Region of Interest (ROI) was circular with diameter of nearly 2 mm.

III. RESULTS

Fig. 5 shows MRI images using T1-w FSE of a lesion deep in the brain (*in vitro*). The length of the lesions is smaller than expected possibly due to the reflection caused by the trapped bubbles. Fig. 6 shows the lesion deep in brain *in vivo* and demonstrates that good penetration of HIFU in brain can be achieved if no bubbles are present.

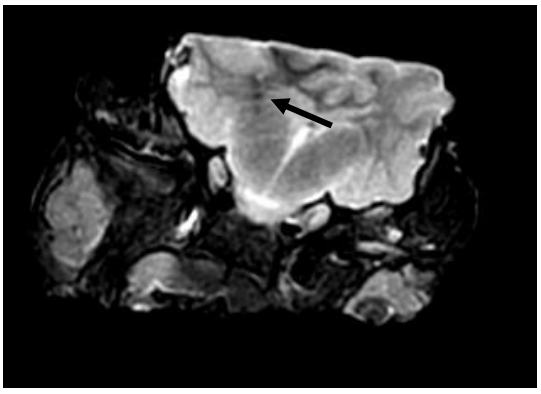

Fig. 5 MRI image using T1-w FSE in vitro.

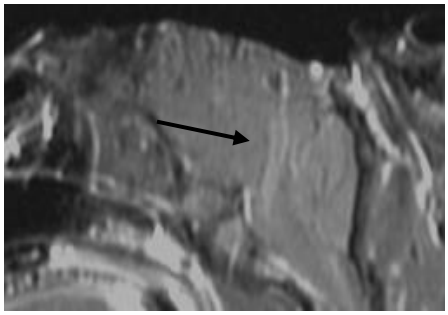

Fig. 6 MRI image using T1-w FSE in vivo.

IV. DISCUSSION

Previous literature ([9-10]) demonstrated that lesions can be monitored with excellent contrast in rabbit brain (in vivo) using T1-w FSE with TR=500 ms. The lesions imaged in the previous studies and also in this study appeared bright with T1-w FSE, whereas brain tissue appeared gray. However in the previous studies only thermal lesions were shown. In this paper we have explored extensively the use of MRI to image both lesions created under thermal mechanisms and mechanisms that create bubbly lesions (cavitation or boiling).

The signal intensity of the brain tissue is homogeneous using T1-w FSE, and therefore the contrast with thermal lesions or with bubbly lesions is excellent.

Both T1-w FSE and T2-w FSE were able to detect lesions. This advantage is attributed to the significant difference in signal intensity between the thermal or bubbly lesions and brain tissue. It was observed that bubbly lesions appear darker than thermal lesions. Bubbly lesions appear dark, due to the air spaces resulting from cavities. This paper demonstrates that non-degassed excised tissue is a good model for easily initiating cavitation. This model of cavitation might not be of any significant for clinical use since the cavitation threshold in live tissue is very different from the threshold in the in vitro tissue. However, this model of initiating cavitation is very useful for the purpose of studying the MRI appearance of bubbly lesions. Cavitation is initiated if a blood vessel (which might include trapped bubbles) is targeted.

The length of the lesions measured parallel to the ultrasonic beam (i.e. deep in the brain) was much higher than the length *in vitro*, proving that the penetration in the *in vitro* brain is limited by reflection due to trapped bubbles in the blood vessels.

ACKNOWLEDGEMENTS

The work was supported by the Research Promotion Foundation (RPF) of Cyprus under the contract ΕΠΙΧΕΙΡΗΣΕΙΣ/ΕΦΑΡΜ/0308/01.

REFERENCES

[1]. Fry W, Mosberg W, Barnard J, Fry F. (1954) Production of focal destructive lesions in the central nervous system with ultrasound. J Neurosurg 11:471-478.

[2]. Lele PP. (1962) A simple method for production of trackless focal lesions with focused ultrasound. J. Physiol. 160:494-512.

[3]. Fry F. and Johnson LK., (1978) Tumor irradiation with intense ultrasound. Ultrasound Med. Biol. 4(4):337-41.

[4]. Britt RH, Lyons BE, Pounds DW, Prionas SD (1983) Feasibility of ultrasound hyperthermia in the treatment of malignant brain tumors. Med Instrum. 7(2):172-7.

[5]. Guthkelch AN, Carter LP, Cassady JR, Hynynen KH, Iacono RP, Johnson PC, Obbens EA, Roemer RB, Seeger JF, Shimm DS, (1991)Treatment of malignant brain tumors with focused ultrasound hyperthermia and radiation: results of a phase I trial, J Neurooncol. 10(3):271-84.

[6]. Vykhodtseva NI, Hynynen K, Damianou C. (1994) Pulse duration and peak intensity during focused ultrasound surgery: theoretical and experimental effects in rabbit brain in vivo. Ultrasound Med Biol. 20(9):987-1000.

[7]. Hynynen K, Vykhodtseva NI, Chung AH, Sorrentino V, Colucci V, Jolesz FA. (1997) Thermal effects of focused ultrasound on the brain: determination with MR imaging. Radiology 204(1):247-53.

[8]. Vykhodtseva N, Sorrentino V, Jolesz FA, Bronson RT, Hynynen K. (2000) MRI detection of the thermal effects of focused ultrasound on the brain. Ultrasound Med Biol 26(5):871–880.

[9]. Hynynen K. McDannold N. Vykhodtseva N. Jolesz F. (2001) Noninvasive MR Imaging–guided Focal Opening of the Blood-Brain-Barrier in Rabbits, Radiology 230:640-646.

[10]. Hynynen K. , McDannold N. , Martin H. , Jolesz F., Vykhodtseva N. (2003) The threshold for brain damage in rabbits induced by bursts of ultrasound in the presence of an ultrasound contrast agent (optison) Ultrasound in Med. & Biol. 29 (3): 473–481.

[11]. Hynynen K., McDannold N., Sheikov N.,Jolesz F. , Vykhodtseva N. (2005) Local and reversible blood–brain barrier disruption by noninvasive focused ultrasound at frequencies suitable for trans-skull sonications NeuroImage 24:12–20.

[12]. Stewart EA, Rabinovici J, Tempany CM, Inbar Y, Regan L, Gostout B, Hesley G, Kim HS, Hengst S, Gedroyc WM. (2006) Clinical outcomes of focused ultrasound surgery for the treatment of uterine fibroids, Fertil Steril. 85(1):22-9.

[13]. Hynynen K, Darkazanli A, Damianou DC, Unger E, Schenck JF. (1992) MRI-guided ultrasonic hyperthermia, RSNA meeting.

[14]. Hynynen K, Damianou CA, Colucci V, Unger E, Cline HH, Jolesz FA. (1995) MR monitoring of focused ultrasonic surgery of renal cortex: experimental and simulation studies. Journal of Magnetic Resonance Imaging 5(3):259-66.

[15]. Christakis Damianou, M. Pavlou, O. Velev, K. Kyriakou, M. Trimikliniotis (2004) High intensity focused ultrasound ablation of kidney guided by MRI Journal of Ultrasound Med Biol 30 (3):397-404.

[16]. Rowland IJ, Rivens I, Chen L, Lebozer CH, Collins DJ, ter Haar GR, (1997) Leach MO., MRI study of hepatic tumours following high intensity focused ultrasound surgery. British Journal of Radiology 70:144-53.

[17]. Rouviere O, Souchon R, Salomir R, Gelet A, Chapelon JY, Lyonnet D. (2007) Transrectal high-intensity focused ultrasound ablation of prostate cancer: Effective treatment requiring accurate imaging, Eur J Radiol, 63(3):317-27.

[18]. Pisani L, Ross A, Diederich C, Nau W, Sommer F, Glover G, Butts K., (2005) Effects of spatial and temporal resolution for MR image-guided thermal ablation of prostate with transurethral ultrasound. J Magn Reson Imaging 22(1):109-18.

[19]. C. Damianou,MRI positioning system for ultrasound brain surgery, WO/2007/082495.

[20]. Lele P Effects of ultrasound on solid mammalian tissues and tumors in vivo, (1987) Plenum publishing corporation 275-306.

[21]. Damianou C. (2003) In vitro and in vivo ablation of porcine renal tissues using High Intensity focused Ultrasound Journal of Ultrasound in Medicine and Biology 29 (9):1321-1330.